Zero field magnetoresistance peaks in open quantum dots: weak localization or a fundamental property?

1999 J. Phys.: Condens. Matter 11 4657

(http://iopscience.iop.org/0953-8984/11/24/307)

J. Phys.: Condens. Matter **11** (1999) 4657–4664. Printed in the UK PII: S0953-8984(99)98705-2

Zero field magnetoresistance peaks in open quantum dots: weak localization or a fundamental property?

R Akis, D Vasileska, D K Ferry and J P Bird

Center for Solid State Electronics Research, Arizona State University, Tempe, AZ 85287-5706, USA

Received 26 October 1998, in final form 15 March 1999

Abstract. Performing numerical simulations of open quantum dots, we reproduce the zero field resistance peaks seen experimentally, a phenomenon previously attributed to weak localization. Our results show however that these peaks can have a different origin, involving conductance resonances that reflect the underlying spectrum. Even with ensemble averaging, we find that the shape of the resistance peak can be more of a probe of these resonances than of the dynamics of the dot.

A common feature found in experiments on quantum dots is a peak in the resistance at zero magnetic field. In one theory [1], these peaks have been attributed to weak localization arising from interference between back-scattered trajectories. This theory also predicts that the shape of the peak depends on whether the cavity dynamics is chaotic or regular. Two important aspects of this theory are: (i) it is valid for cases where $\hbar/\tau_0$ is large compared to the mean level spacing, τ_0 being the escape time, and (ii) to obtain the lineshapes, an integration over *all* wavenumbers, k, was performed. A large dot with wide openings is required for (i). The implication of (ii) is that any experimental comparison requires that a *large* ensemble average be performed. Attempts at comparison have been made by: considering multiple arrays of similarly configured devices [2], considering individual devices, but averaging over gate voltage [3–6], disrupting the phase coherence by thermal cycling [7, 8], measuring devices at finite temperature [7–9] and constructing devices in which k could be independently varied [10]. However, in many instances, the dots were relatively small and had only a few modes in the quantum point contacts (QPCs). Moreover, apparent agreement with the theory has been achieved by exploring fairly small regions of k space [5–11]. Thus, it was questionable that the above criteria were being satisfied.

The weak localization peak in a chaotic cavity is predicted to take the Lorentzian form [1]:

$$R(B) = R_0 + \frac{\Delta}{[1 + (2B/\alpha\phi_0)^2]} \tag{1}$$

where $R(B)$ is the resistance at magnetic field B, $\phi_0 = h/e$, R_0 is the resistance in the absence of localization, and α^{-1} is a parameter that represents the area enclosed by a typical trajectory (this can be substantially larger than the cavity size). For a regular cavity, a linear lineshape is expected, however there is no formula that can be used for fitting. With regards to the experiments, Chang *et al* [2], found that an ensemble of stadium cavities obeyed equation (1),

0953-8984/99/244657+08$19.50

while a circular ensemble did not. On the other hand, Berry *et al* [5] and Lee *et al* [6] found that circular cavities instead yielded Lorentzian lineshapes. Studying a number of different cavity shapes, Lee *et al* [6] found that only a rectangular cavity gave linear behaviour. However, Bird *et al* [7] found that rectangular cavities could yield *both* Lorentzian and linear lineshapes. These apparently contradictory observations raise the questions: is a Lorentzian lineshape a reliable indicator of chaos? If not, could there be another explanation for the observed lineshapes?

To resolve this issue, in this paper we present results that suggest that the presence of the zero field resistance peaks may be attributed to a phenomenon other than weak localization. In the semi-classical theory of dots, the energy spectrum is given by the *closed* trajectories [12]. In our simulations, we obtain zero field peaks, but find that they arise from the fundamental properties of this energy spectrum, and not from weak localization. We consider two situations: a square dot for which we have calculated the conductance, G against energy, E, and magnetic field, B, and a dot with a realistic soft potential obtained self-consistently, permitting us to study $G(V_g, B)$, where V_g is applied gate voltage. For the square dot, the dynamics should be regular, but for the realistic dot profile, the potential rounding should yield chaotic boundary scattering [13]. We find that $G(E, B)$ and $G(V_g, B)$ are prominently striated by lines of resonances. These resonances tend to correspond to states scarred by periodic orbits [14, 15]. Performing ensemble averages over G, we obtain resistance peaks that are strikingly similar to those seen experimentally. With regards to the peak lineshape, we find that the dot geometry appears to be of secondary importance. In particular, a transition between Lorentzian and linear lineshape can be obtained in the square dot and we find that both dots give similar results, when suitable averages are taken.

Our simulations were performed on a discrete lattice using a numerically stabilized variant of the transfer matrix approach [16]. The dot is enclosed inside a waveguide which extends a finite number of lattice sites in the transverse (y) direction. The structure is broken down into a series of slices along the longitudinal (x) direction. Imposing an electron flux from the left, one translates across successive slices and, on reaching the end, one obtains the transmission coefficients which enter the Landauer–Büttiker conductance formula. For the realistic confining potential, the simulated structure consists of a split gate sitting on top of a GaAs–AlGaAs heterostructure. Finding the solutions for the potential requires solving the 3D Poisson equation, then solving the 1D Schrödinger equation and reconciling the potential and electron density in an outer iteration for self-consistency [17, 18].

In figure 1, we show how the conductance for an open quantum dot relates to the closed dot spectrum. A generic formula for G reveals the relationship to the density of states (DOS) [19]:

$$G \sim \frac{e^2}{2m^2} \int \frac{\mathrm{d}^2 p}{(2\pi)^2} p^2 \int_0^\infty \frac{\mathrm{d}E}{2\pi} [A(p, E)]^2 \left(-\frac{\mathrm{d}f_{FD}}{\mathrm{d}E} \right) \tag{2}$$

where $A(p, E)$ is the spectral density (the integral over $A(p, E)$ with respect to momentum, p, yields the DOS). Hence, a study of G should show a correspondence to the DOS and the dot energy levels. Figure 1(a) shows part of the spectrum as a function of B for a *closed* square dot of side 0.3 μm. The spectral lines form a 'winged' pattern with an 'eye' in the centre. Figure 1(b) shows the corresponding conductance, $G(E, B)$ for an open dot (the configuration is shown in the inset of figure 1(c)). Here the QPCs allow two modes. $G(E, B)$ clearly shows the influence of the closed dot DOS, as the basic pattern is reproduced. The match is not exact since opening the dot broadens the energy levels. Importantly, this broadening is *not uniform*. The QPCs create a collimation effect that preferentially excites particular orbits [14, 20, 21]. Moreover, certain orbits are automatically disallowed by the presence of the QPC openings.

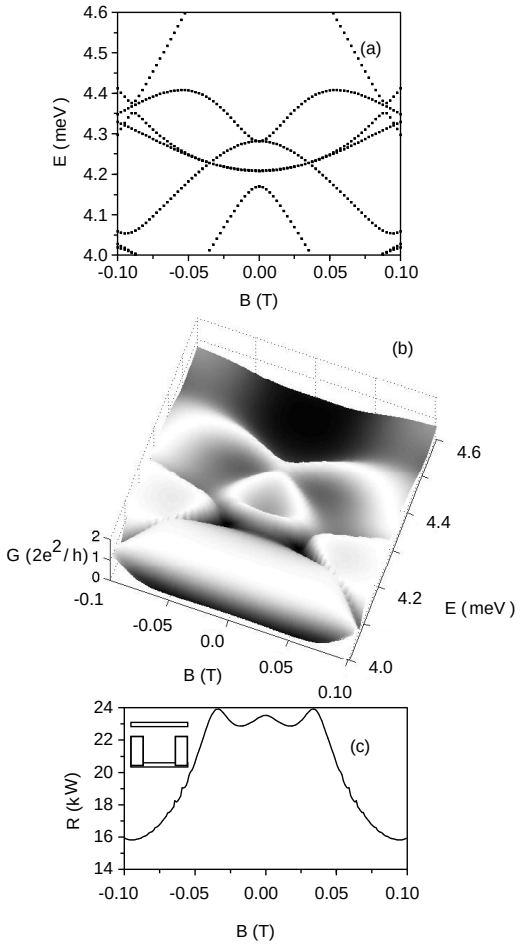

Figure 1. (a) E against B for a closed 0.3 μm square dot. (b) $G(E, B)$ for a corresponding open dot. (c) R against B, where R is the resistance obtained by averaging over all conductance traces in (b). Inset: the open dot configuration.

This orbit selection is crucial in determining which closed dot states survive [20, 21]. Thus, certain spectral lines are very strongly reflected by G, while others are weak or completely absent (a uniform broadening model [22] for the coupling from the QPCs to the dot states will not pick up this subtlety). Along many of the spectral lines, resonant minima occur in close proximity to maxima. This is because resonances tend to have a Fano lineshape that combines both in open structures [23]. A deep trough occurs between 4.2 and 4.3 meV, where two spectral lines are degenerate. Figure 1(c) shows the resistance, R, obtained after ensemble averaging over all the traces shown in figure 1(b). Features in R clearly can be related back to the underlying DOS. The small central peak results from the 'eye' while the side peaks result from the minima that occur at two crossings of spectra lines. The dominant feature is a plateau resulting from the trough.

Figure 2(a) shows $G(E, B)$ for this dot, but over a larger energy range. Lighter shading corresponds to higher G. Note that many features recur quasi-periodically. Specifically, 'diamond' patterns are formed by sets of angled, almost parallel, lines of resonances. Inside

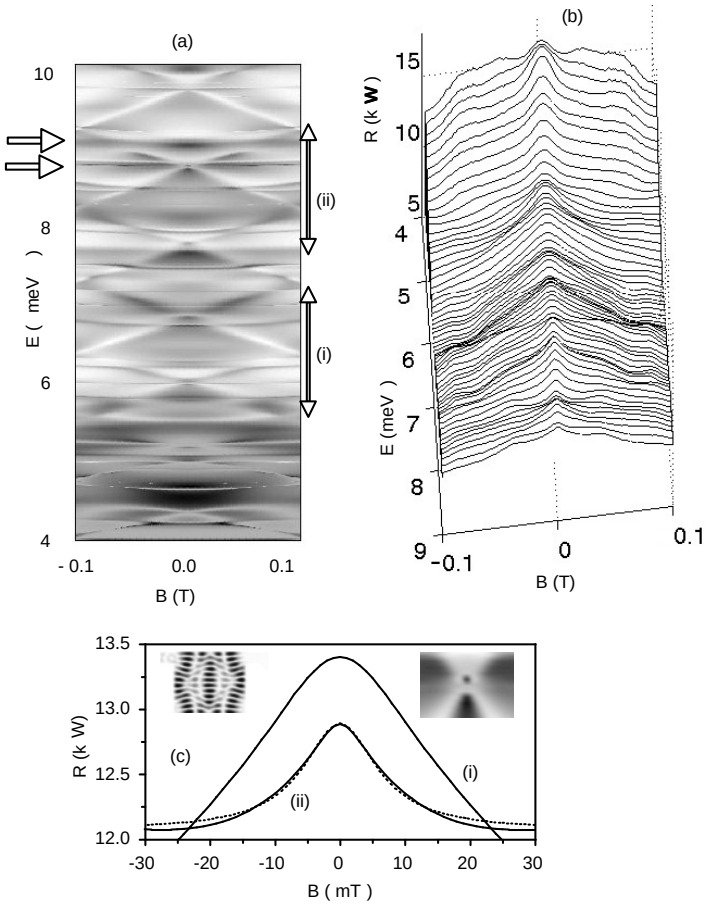

Figure 2. (a) $G(E, B)$ is plotted for the 0.3 μm square dot. (b) R against E and B, where the traces were obtained by averaging G in (a) over a 1.5 meV window. (c) R against B for two traces obtained by averaging over the ranges shown in (a). The dotted line is a Lorentzian fit.

the diamonds, triangular patterns occur due to crossing resonance lines. It is clear that the resistance peak at $B = 0$ is not a general feature of the individual traces. Ensemble averages are required to obtain a peak in all cases. Figure 2(b), a plot of R against E and B, shows a result of such a calculation. Each trace was obtained by averaging $G(E, B)$ over a window of 1.5 meV. Importantly, *this window is larger than the period of the recurring diamond pattern*. If the window is small compared to this period, *then a peak will not always result*. The higher resistance traces shown in the upper part of figure 2(b) correspond to averages over the lower ranges of figure 2(a). While the peak is now universal, its lineshape clearly evolves with E. Traces (i) and (ii) shown in figure 2(c) were obtained by averaging over the ranges indicated in figure 2(a). Trace (i) appears linear, the prediction [1] for regular structures. Trace (ii) can be fitted (the dotted line) to the Lorentzian form of equation (1), using $R_0 = 12.07$ kΩ, $\Delta = 0.82$ kΩ and $\alpha\phi_0 = 6.82$ mT. Here, $\alpha^{-1} \sim 7$ A, where A is the dot area. While a transition from linear to Lorentzian lineshapes has been induced in experimental studies of small dots [7, 8], and has been attributed to a transition from regular to chaotic scattering, such a scattering change is not possible in figure 2(c), in which the dot geometry is constant. Rather the reason for the lineshape change is that we are now averaging over a different energy

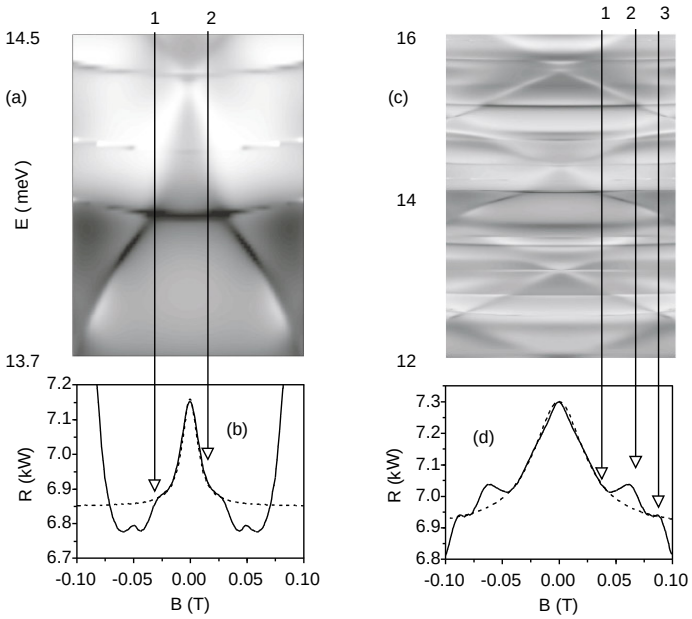

Figure 3. (a) $G(E, B)$ is plotted for the 0.3 μm square dot. (b) R against E and B, resistance average over (a). (c) $G(E, B)$ again, but for a larger range. (d) R against B, the resistance average over (c). The dotted lines in (b) and (d) are Lorentzian fits.

range, so different spectral features get mapped into the resistance. With regards to trace (ii), a 'hole' in G at ∼8.71 meV (lower arrow) is primarily responsible for the Lorentzian peak. This feature is enlarged in the right inset and is an example of resonant *reflection* from a quasi-bound state (the wave function in the left inset). Such resonant reflections were first noted for T-stub structures [24]. The trough indicated by the upper arrow creates the plateau. The features in region (i) are softer, leading to the more uniform lineshape.

Figure 3 shows how increasing the averaging range changes lineshape. Figure 3(a) shows $G(E, B)$ for $13.7 < E < 14.5$ meV. This corresponds to only a portion of a diamond. Evident here is a triangular feature whose bottom is defined by a deep resonance line and is cut in half by a second line creating an inner triangle. The averaged resistance in figure 3(b) shows a peak and two shoulder-like features that coincide with the bottom corners of the larger triangle (arrow 1), while the inflection points where the shoulders emerge correspond to the corners of the inner triangle (arrow 2). Shoulders are a common feature seen experimentally (for example, see figure 1(b) of [2]). The dotted line is the almost perfect Lorentzian fit, with $R_0 = 6.85\,\mathrm{k}\Omega$, $\Delta = 0.4\,\mathrm{k}\Omega$ and $\alpha_0 = 16\,\mathrm{mT}$. Here, $\alpha^{-1} \sim 3\,A$. Figure 3 (c) shows $G(E, B)$ for $12 < E < 16$ meV, which contains the smaller range as a subset. In this case, several diamonds are included and the resulting averaged lineshape has to a large degree saturated as a result of their quasi-periodicity. The averaged resistance (figure 3(d)) indicates that other features are dominant over the larger range. The inflection points are gone and there is barely a trace of the original shoulders (arrow 1). New shoulders coincide with other resonance crossings (arrows 2 and 3). The peak is now much wider and *appears* to be *linear*. This however is a plotting artifact—this peak can be fitted (dotted line) very well using $R_0 = 6.9$ kΩ, $\Delta = 0.31$ kΩ and $\alpha\phi_0 = 55$ mT. Now, $\alpha^{-1} \sim A$. Thus, significantly different values of α^{-1} result by changing the averaging range. Again, since dot geometry is fixed, it is unlikely that a change

in dynamics accounts for this. Experimentally, the cavities of Berry *et al* [5] gave $\alpha^{-1} \sim 3\ A$, while other authors found $\alpha^{-1} \sim A$ [2, 6, 7]. Importantly, a narrow peak can also be obtained in our simulations by using the larger range, but doing an incomplete average that skips over many traces. In experiment, such limited sampling can be unavoidable (Berry *et al* [5] for example averaged over only five traces for their results).

Referring back to the linear peak shown in figure 2(c), like all the other lineshapes we have shown, it has a rounded top. However, it appears linear because the conductance resonances in that case contribute so weakly that they do not appear to create shoulders (they are present, but are barely noticeable). From the progression shown in figure 2(b), it appears that it is the rise of such shoulder features that turns a linear peak into a Lorentzian. Since resistance traces will generally have rounded features, it makes it exceedingly difficult to truly distinguish between the two cases.

In figure 4, we show results for the realistically modelled dot. For the heterostructure, we used the same parameters as in an earlier simulation [17]. The simulated top gates define a dot of side 0.4 μm with QPCs 0.1 μm wide. Applying a bias reduces dot size and QPC width. A typical self-consistent profile is shown in figure 4(a) and has a bowl shape expected to create chaotic behaviour classically. While the effective size changes with V_g, this basic shape does not, so a change in dynamics is not expected. With $E = 15$ meV in the external reservoirs, the QPCs support five or six modes over the bias range considered. In figure 4(b), we plot $G(V_g, B)$. As with $G(E, B)$, striations which reflect the underlying DOS are present, forming a 'honeycomb' of diamonds. The averaged resistance is shown in figure 4(c). Similar to figure 3(d), the energy averaged peak appears linear but can be fitted using equation (1) (dashed line, $R_0 = 2.59$ kΩ, $\Delta = 0.095$ kΩ and $\alpha\phi_0 = 35$ mT). Here, $\alpha^{-1} \sim A$, a result similar to that obtained above for the square. As above, shoulders appear that are a cumulative result of the resonances that occur at major non-zero line crossings (note the arrows) and that averaging over several diamonds has caused some convergence of this lineshape. What is different about this ostensibly chaotic dot? While sharing some similar qualitative features, the underlying striation pattern is clearly different. Moreover, the sets of states that yield these striations in the two geometries can also be quite different. There are resonant states that occur in the rounded geometry that are impossible in the square geometry and vice versa.

The conventional view is that zero field resistance peaks are weak localization effects [1]. While formula (1) was obtained after averaging, these effects, if real, should be present even without averaging. In traces where the peak does not appear, the contention was that it was being obscured by fluctuations (i.e. the resonances we have shown) and that the effect of the ensemble averaging was to average these *out* to reveal an underlying peak [1]. We argue that the opposite is happening. There is no underlying peak and ensemble averaging simply averages these fluctuations *in*. Recall that the plateau in figure 1(c) was generated by a trough in G. While conductance minima obviously occur along individual spectral lines, they tend to be more strongly weighted the more states are involved (it was the coincidence of spectral lines that yielded the strongest features in figure 1(b)). The location where there is the greatest density of spectral lines coinciding is at $B = 0$, the point of *maximum degeneracy* (there are two $B = 0$ states for each $B \neq 0$ state). Finite B lifts the degeneracy (see figure 1(a)). When shoulder peaks are present, these coincide with the positions of major line crossings, where a local increase in degeneracy has lead to deeper relative minima in G. It is worth reiterating an important point made above, namely that to obtain a zero field peak in all instances requires that the averaging be done over a range larger than the diamond resonance patterns in the conductance. This is compelling evidence that the peaks are strongly tied to the presence of resonances at zero field.

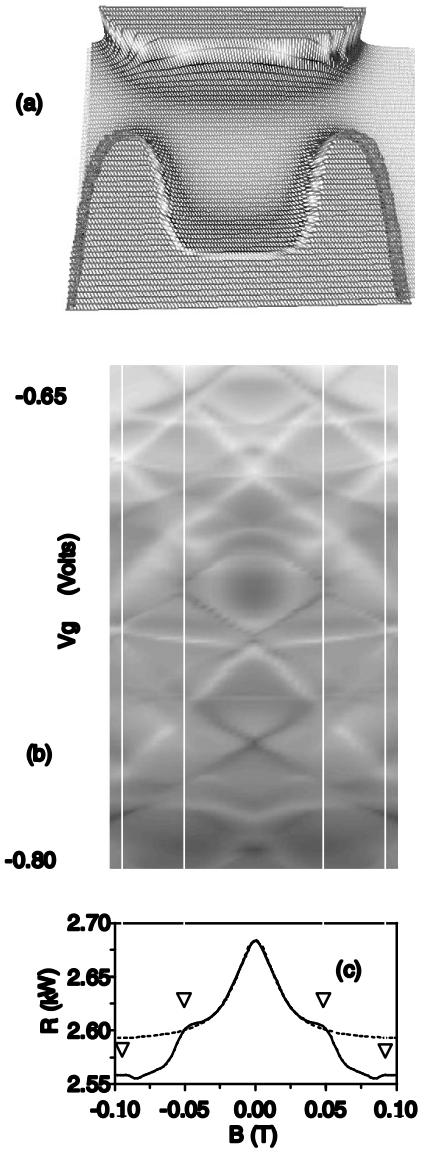

Figure 4. (a) A potential obtained self-consistently. (b) $G(V_g, B)$ for the self-consistently modelled dot. (c) R against B, where R was obtained by averaging over all of (b). The dotted line is a Lorentzian fit.

In summary, we have shown that the conductance of a ballistic quantum dot displays features that reflect the details of its underlying spectrum. Energy averaging does not destroy this dependence. Instead, zero field peaks and corresponding structure such as shoulders appear to be a reflection of conductance resonances and not an additive effect such as weak localization. Since our simulations do not generally meet the criteria mentioned in the first paragraph, we cannot conclude that the weak localization theory is invalid in that limit. However, it is clear that the resonance phenomena we have discussed can cause virtually indistinguishable effects. Moreover, shoulder side peak features, commonly observed in experiment, have *no* explanation

in the weak localization theory. Various resistance lineshapes and linewidths, including both linear and Lorentzian shapes, can be obtained in a *single* dot. Comparing regular and chaotic geometries, we obtain qualitatively similar results. As such, the mere presence of a particular lineshape cannot be used to ascertain whether the dynamics is regular or chaotic, even with averaging. This conclusion is consistent with the varied results obtained in recent experiments.

Acknowledgments

We acknowledge the financial support of ONR and DARPA.

References

[1] Baranger H U, Jalabert R A and Stone A D 1993 *Phys. Rev. Lett.* **70** 3876
Baranger H U, Jalabert R A and Stone A D 1993 *Chaos* **3** 665
[2] Chang A M, Baranger H U, Pfeiffer L N and West K W 1994 *Phys. Rev. Lett.* **73** 2111
[3] Marcus C M, Rimberg A J, Westervelt R M, Hopkins P F and Gossard A C 1992 *Phys. Rev. Lett.* **69** 506
[4] Chan I H, Clarke R M, Marcus C M, Campman K and Gossard A C 1995 *Phys. Rev. Lett.* **74** 3876
[5] Berry M J, Katine J A, Westervelt R M and Gossard A C 1994 *Phys. Rev.* B **50** 17 721
[6] Lee Y, Faini G and Mailly D 1997 *Phys. Rev.* B **56** 9805
[7] Bird J P, Olatona D M, Newbury R, Taylor R P, Ishibashi K, Aoyagi Y, Sugano T and Ochiai Y 1995 *Phys. Rev.* B **52** 14 336
[8] Bird J P *et al* 1997 *Chaos Soliton Fract.* **8** 1299
[9] Taylor R P, Newbury R, Dunford R B, Coleridge P T, Sachrajda A S and Adams J S 1995 *Phys. Rev.* B **51** 9801
[10] Keller M W, Mittal A, Sleight J W, Wheeler R G, Prober D E, Sacks R N and Shtrikmann H 1995 *Phys. Rev.* B **52** R14 336
[11] Taylor R P *et al* 1997 *Phys. Rev. Lett.* **78** 1952
[12] Brack M and Bhaduri R K 1997 *Semiclassical Physics* (Reading, MA: Addison-Wesley)
[13] Ketzmerick R 1996 *Phys. Rev.* B **54** 10 841
[14] Akis R, Ferry D K and Bird J P 1996 *Phys. Rev.* B **54** 17 705
[15] Akis R, Ferry D K and Bird J P 1997 *Phys. Rev. Lett.* **79** 123
[16] Usuki T, Saito M, Takatsu M, Kiehl R A and Yokoyama N 1995 *Phys. Rev.* B **52** 8244
[17] Okubo Y, Ochiai Y, Vasileska D, Akis R, Ferry D K, Bird J P, Ishibashi K, Aoyagi Y and Sugano T 1997 *Phys. Lett.* A **236** 120
[18] Akis R, Vasileska D, Ferry D K, Bird J P, Okubo Y, Ochiai Y, Ishibashi K, Aoyagi Y and Sugano T 199? *Physica* B **249–251** 353
[19] Mahan G 1990 *Many-Particle Physics* (New York: Plenum)
[20] Akis R and Ferry D K 1998 *Semicond. Sci. Technol.* **13** A18
[21] Ferry D K, Akis R, Pivin D P, Bird J P, Holmberg N, Badrieh F and Vasileska D 1998 *Physica* E **3** 137
[22] Persson M, Pettersson J, von Sydow B, Lindelof P E, Kristensen A and Berggren K F 1995 *Phys. Rev.* B **52** 8921
[23] Porod W, Shao Z and Lent C S 1993 *Phys. Rev.* B **48** 8496
[24] Sols F, Macucci M, Ravaioli U and Hess K 1989 *Appl. Phys. Lett.* **54** 350